Study of the Efficiency and Resolution of the New sMDT Chambers at the ATLAS Experiment

Ethan Cannaert

April 13, 2018

Abstract

Abstract: During the 2016/2017 winter shutdown at the Large Hadron Collider, 12 new sMDT (small monitored drift tube) chambers were installed in the barrel of the ATLAS detector. The drift tubes that make up these chambers have half the radius of normal drift tubes and as such are better suited for the high rates of radiation that will become common as the LHC upgrades to higher luminosities. As sMDT chambers are a fairly new technology, there is still much unknown about their performance at the LHC. This thesis looks to evaluate the efficiency and performance of the new sMDT chambers using beam data collected by the ATLAS experiment during 2017. In doing this, a serious issue involving muon track reconstruction of sMDT chambers was discovered, which will also be discussed.

1 Background

The Large Hadron Collider The Large Hadron Collider (LHC), built by the European Organization for Nuclear Research (CERN) near Geneva, Switzerland, is currently the world's largest and most powerful particle accelerator. Since its first collisions in 2009, the LHC has expanded our understanding of fundamental particle physics by exploring proton-proton (p-p) collisions at groundbreaking luminosity and energy around its 17 km circumference. The LHC provides p-p collisions at a center-of-mass energy of $\sqrt{s} = 13$ TeV and luminosity of $10^{34}\ cm^{-2}s^{-1}$ at a rate of 40 MHz, however it has the potential to deliver luminosities as high as 7.5 x $10^{34}\ cm^{-2}s^{-1}$. This potential will be reached in multiple steps, the first of which will take place during long shutdown 2 between 2019 and 2020 during which the luminosity will be increased to above 2 x $10^{34}\ cm^{-2}s^{-1}$. This large increase in luminosity means an increase of particle radiation that will require the installation of new detector technologies that can function under these conditions. The planned increase in luminosity will unlock further opportunities to study and answer many of the unsolved questions in particle physics, such as whether Supersymmetry is realized in nature, whether there exist extra dimensions as is theoretically postulated, and the nature and origin of dark matter.

Distributed throughout the circumference of the LHC are seven experiments located at one of the four beam crossing points. The specialized experiments are LHCb, which focuses on the detection of charge conjugation parity symmetry (CP symmetry) of bottom quarks,

ALICE, which studies heavy ion collisions, TOTEM, which looks to measure scattering and cross section of particles, LHCf, which is involved with cosmic ray physics, and MoEDAL, which searches for magnetic monopoles. Aside from these, there are two general-purpose detectors, ATLAS and CMS, both of which were responsible for the discovery of the Higgs boson in 2012.

The ATLAS Experiment The ATLAS experiment is the largest of the seven experiments and is currently being used for multiple physics purposes, including studying the decay and properties of the Higgs boson, identifying dark matter candidates, and the search for extra dimensions. While the ATLAS experiment is closely related to the CMS experiment in terms of physics goals, they employ different technologies and have different magnet systems.

The ATLAS experiment is composed of three detectors: the inner detector, the calorimeters, and the muon spectrometer. The inner detector sits close to the beam axis out to a radius of 1.2 m. It employs three main technologies: the inner pixel detector consisting of detecting silicon pixels that provide very accurate tracking, the semi-conductor tracker consisting of strips of silicon semi-conductors that does most of the overall tracking, the transition radiation tracker made of very small drift tubes that constitute a "straw tracker", and a transition radiation detector. Additionally, the inner detector is completely surrounded by a 2 T solenoid magnet that causes particles that travel through it to have curved trajectories. The inner detector's main role in the ATLAS detector is to measure the trajectory and momenta of charged particles. This is accomplished by measuring the sagitta (amount of bending) of the curved trajectories of the charged particles that move through each layer, from which momenta can be determined.

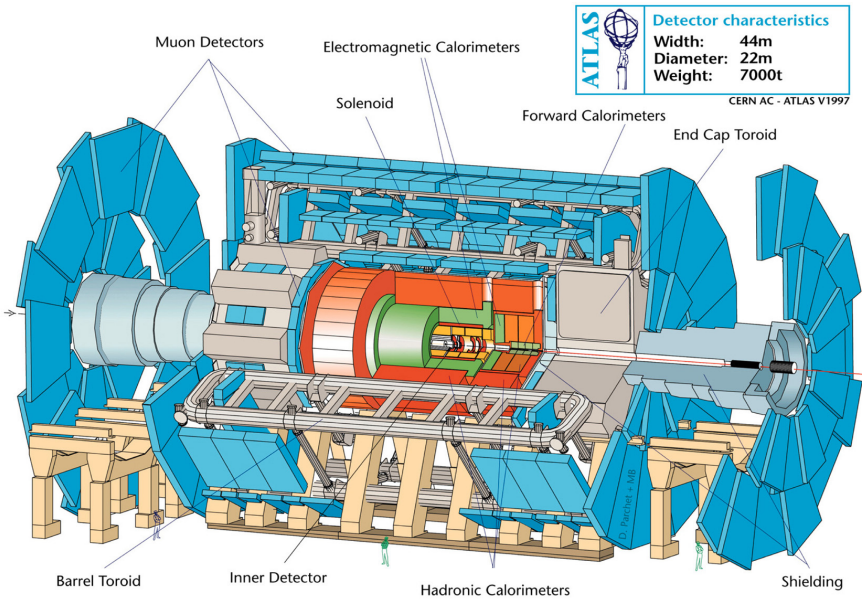

Figure 1: The setup of the ATLAS experiment and its three main detectors. CERN, 1997 [1]

There are two calorimeters, electromagnetic and hadronic, that measure the distance of penetration of particles through each detector in order to measure their energies. The electro-

magnetic calorimeter uses liquid argon to absorb the energy of electrons by completely stopping each particle by electromagnetic interactions. The energy of photons passing through the calorimeter is also measured by measuring the electron-positron pairs that photons convert into. Using the known properties of liquid argon, the penetrative depth of a particle through the detector allows for very very accurate measurements of particle energies. The hadronic calorimeter, located on the outside of the electromagnetic calorimeter, measures the energy of hadrons, which are particles that are made of quarks that interact via the strong force, using over 500,000 plastic scintillator tiles.

Lastly, the muon spectrometer employs a strong toroidal magnet that bends the trajectories of charged particles, and several types of chambers in order to calculate the momentum of muons. Muons are the second generation lepton partner to the electron with a rest mass of 105.7 MeV/c^2, and are able to make it through the inner detector and calorimeters. The detection of muons is of particular interest because high-energy muons can be the result of the decay of the Higgs boson and other massive particles being studied at the LHC.

As discussed before, the luminosity of the LHC is currently around $1.6 \times 10^{34}\ cm^{-2}s^{-1}$ with a p-p rate of 40 MHz. Due to technological limitations, data can only be recorded at around 100 Hz, so high-precision triggering is required in order to extract the events with the highest potential for new physics. This is achieved by a three level triggering system where the level-1 trigger cuts down the number of recorded events by a factor of 100 in under 1.6 μs using a rough calculation for particles with high transverse momentum (p_t), and the last two trigger levels each reduce the number of events by a further factor of 10,000 to only retain the most significant collision events.

The Muon Spectrometer The muon spectrometer makes up the outermost part of the ATLAS experiment, spanning from a radius of 4.25 meters from the interaction point out to 11 meters. It consists of a barrel surrounding the beam axis and two endcaps perpendicular to it. The barrel is divided into three layers at approximately 5 m, 7.5 m, and 10 m from the beam line. Additionally, there are four different layers of endcaps at varying distances from the interaction point that detect the high level of radiation near the beam line. The main function of the muon spectrometer is to measure and track charged particles, mainly muons, that make it through the inner detector and calorimeters. Overall, the muon spectrometer provides tracking coverage for $|\eta| < 2.7$ where η is the psuedorapidity [1]. Three powerful toroid magnets providing between 1 T·m and 7 T·m of bending power act on these particles and send them along a curved trajectory. Their trajectory is then tracked, and the sagitta is used to determine the momentum.

This achieved by four different technologies: monitored drift tubes (MDT), cathode strip chambers (CSC), resistive plate chambers (RPC), and thin gap chambers (TGC). Cathode strip chambers provide high precision tracking in the first layer of the endcaps with a spatial resolution of approximately 60 μm per CSC layer. 32 CSC's are mounted azimuthally perpendicular to the beam line in the first layer of the end caps where $2 < |\eta| < 2.7$. In this region the rate of radiation is too large for the use of MDT's, but the drift time for electrons in cathode strip chambers is only about 40 ns, which allows the CSC's to have good tracking

[1] η is defined as $-\ln\tan\frac{\theta}{2}$ where θ is the angle between the beam axis and the particle momentum. For reference, $\eta = 0$ refers to the line perpendicular to the beam axis, and $\eta = \infty$ is parallel to the beam axis.

resolution at counting rates as high as 1000 Hz/cm^2. Thin gap chambers occupy the endcaps in several layers in the range $1.05 < |\eta| < 2.7$ (though the range for triggering is only to $\eta = 2.4$). These chambers provide both triggering and second coordinate (the coordinate in the non-bending direction) calculation for the CSC chambers. Each of the over 3500 chambers is made from a plane of wires kept at a positive voltage layered between two grounded cathode plates, and are measured to have an efficiency of greater than 95% for backgrounds of less than 500 Hz/cm^{-2}.

Monitored drift tubes do the majority of tracking in the muon spectrometer, with 1186 chambers and over 350,000 total drift tubes. MDT chambers surround the barrel in three layers and endcaps in four layers at 16 different azimuthal angles, providing coverage for $\eta < 2.7$ in the outer layers, and $\eta < 2.0$ for the innermost layer where the CSC's are installed in the endcap region. Mounted to the two out layered barrel MDT chambers are resistive plate chambers, which are detectors made of two parallel electrode plates that utilize a gas mixture of $C_2H_2F_4/C_4H_{10}/SF_6$ (94.7%, 5.0%, 0.3%) in order to make fast p_t measurements. Over 600 of these RPC's provide triggering in the range $\eta < 1.05$. Additionally, they provide second coordinate calculations for the MDT chambers along the length of each tube.

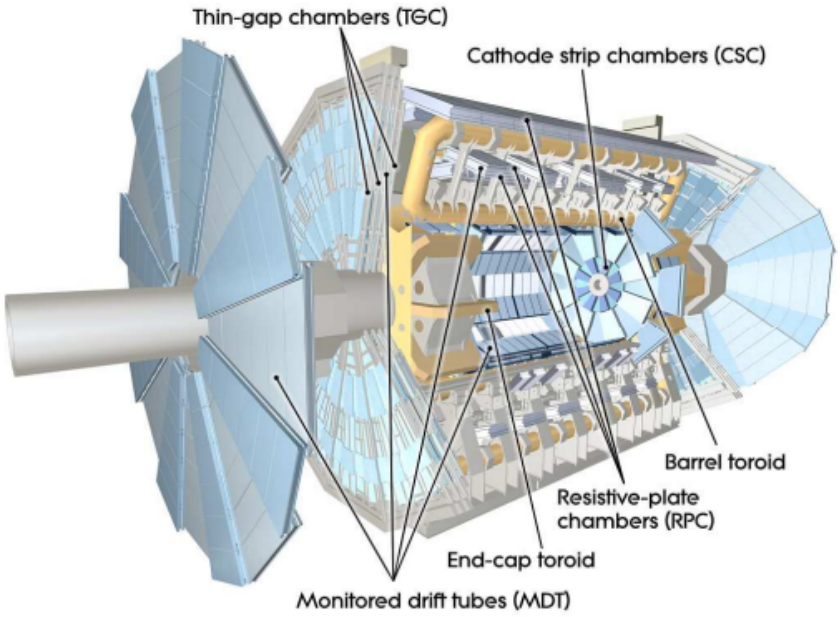

Figure 2: The technologies being utilized in the muon spectrometer. The resistive plate chambers and thin gap chambers provide triggering for the monitored drift tube and cathode strip chambers, which in turn provide precision tracking of charged particles [1]

Monitored Drift Tubes (MDT) Within the muon spectrometer, the dominant tracking technology is the monitored drift tube. Monitored drift tube chambers provide a very reliable and highly accurate method for tracking charged particles. The drift tubes used in these chambers are made from aluminum tubes with a diameter or 29.97 mm and are filled with an Ar/CO_2 mixture (93%/7%) at a pressure of 3 bars. The general concept is that charged particles pass through these tubes and ionize the gas inside them, causing electrons to cascade

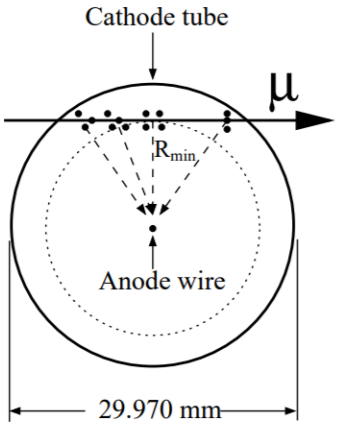

Figure 3: Cross section of a charged particle passing through a drift tube. The charged particle ionizes electrons in the gas that drift to the anode wire at the center [1]

toward the center of the tube and then be collected by a gold-plated tungsten-rhenium wire of diameter 50 μm located at the center. The collected charge is then measured by readout electronics and digitized before being recorded if that particular event makes it past the trigger discrimination. The drift time of a hit can be combined with the appropriate RT function, which converts measured drift times to drift radii, in order to obtain a corresponding drift radius for that hit. After data has been collected for a run at the ATLAS experiment, the Athena reconstruction software analyzes it and uses hits on all chambers to construct probable muon trajectories, which are referred to as muon tracks. Additionally, Athena fits shorter tracks for each chamber called "segments" that are made using only hits found on that chamber. There are often multiple hits per event that cross a single tube, and hence an electrical dead time of 790 ns is implemented in order to prevent hits from interfering with each other.

Without irradiation, the resolution of MDT chambers is 83 ± 2 μm, which is close to the resolution that is being found from real beam data from the LHC. This value of resolution given to each chamber is the average value of the plot of spatial resolution as a function of drift radius. Figure 4 gives an example of the plot of spatial resolution at different drift radii made from test beam data, and shows that the resolution is very poor for small drift radii. This is because when particles pass through the tube at small radii, the resulting ionized electrons often do not have enough distance to cause a large enough cascade of secondary electrons to create a signal that is strong enough to make it past the electronics discriminator. Signals from electrons arriving from particles that pass through the tube at larger radii tend to get measured instead. Additionally, the drift speed of electrons is large near the wire, so there is larger uncertainty as to its position than that of slow moving electrons from tube hits near the edge of the tube.

Drift tubes are cemented together in either multiple layers, usually six or eight, separated into two multilayers with a gap in between. Chambers range between 1-6 m in length and 1-2 m in width. Using many tubes in each chamber gives them good physical strength, and also

prevents large-scale failure in the case of a single tube failing. A disadvantage of the tube geometry of drift tubes is that the second coordinate resolutions along the length of the tube are fairly poor in comparison to the radial coordinate resolutions. For segments, the second coordinates are often only accurate on the order of millimeters to centimeters. Another disadvantage of MDT chambers is that their bulky size makes it impossible to mount RPC chambers on the inner barrel chamber.

This particular gas mixture of Argon and CO_2 was chosen because it has a considerably long lifetime in comparison to other comparable gases. Gas mixtures containing hydrocarbons such as methane often have low drift times and linear space-drift time relations, but high rates of radiation cause them to degrade over time and deposit molecular debris on the wire, which interferes with particle detection. For this reason, a gas mixture without hydrocarbons was chosen. The disadvantage of the chosen Ar/CO_2 gas mixture is that it has a non-linear space-drift time relation, and also has a maximum drift time of about 700 ns, corresponding to a muon passing through the drift tube at the tube wall, which is upwards of 50% longer than alternative gases. This large drift time leads to a dramatic decrease in tube resolution at high rates of radiation, as is shown in figure 4. This loss of resolution at high radiation rates is a significant problem in regions of detector that have high counting rates, mainly the endcaps.

sMDT Chambers As the LHC looks to increase the luminosity of its beams in order to search for new physics, the detector technologies of the ATLAS experiment need to evolve to cope with the new levels of radiation that this brings. Building off of studies of how the resolution and efficiency of monitored drift tubes decay with increases in radiation, new small monitored drift chambers (sMDT) have been built to replace certain MDT chambers in areas of high particle flux. The tubes in these new sMDT's use the same gas mixtures and pressures as a normal drift tube, but operate at a voltage of 2760 V, as opposed to 3080 V for MDT chambers, in order to have the same RT functions as MDT's, and have a radius that is half the size (7.5 mm) of a normal MDT tube. The difference in diameter is shown in figure 5. This shortens the maximum drift time to about 175 ns compared to 700 ns for MDT's, which means the electronic dead time is about a factor of four smaller for sMDT's than for MDT's, allowing for sMDT chambers to function at 8 times higher rates than MDT chambers [2]. The comparison of the drift time spectrum plots for both different types of chambers is shown in figure 6.

Another benefit of using smaller tubes is that chambers can be made less physically bulky than MDT chambers. This allows sMDT chambers to be built that can fill in certain areas of the muon spectrometer that other chambers could previously not be installed. During the 2016/2017 winter shutdown, the University of Michigan installed 12 new sMDT chambers, designated "BMG", that filled holes in the geometric acceptance of the barrel that normal MDT chambers were too big to cover. Additionally, two sMDT chambers, designated "BME", were also installed in order to provide tracking coverage to a previously empty region. Another benefit to the smaller size of sMDT chambers is that they free up space in cramped areas of the detector that can then be used to mount triggering chambers.

[2] sMDT chambers have $\frac{1}{4}$ the drift time and $\frac{1}{2}$ the tube radius of MDT chambers, resulting in an eightfold increase in rate capacity.

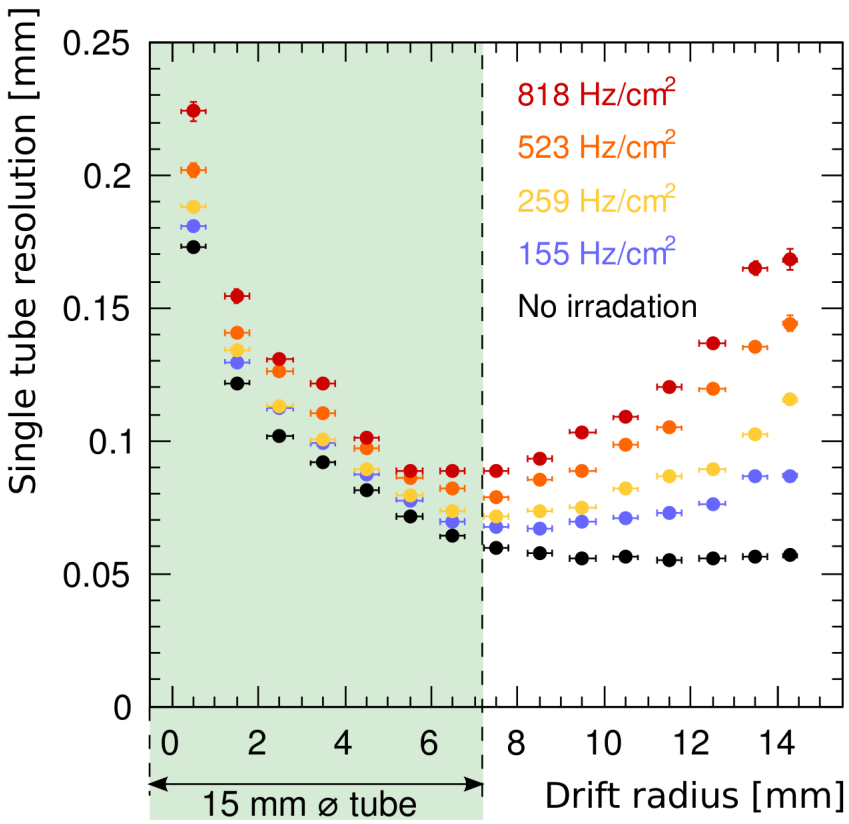

Figure 4: Measured spatial resolution of MDT chambers vs the drift radius at different rates of radiation. Increased radiation resulted in much poorer resolution for drift radii of 7.5 mm and greater. On the other hand, the resolution was much less affected for small drift radii [7].

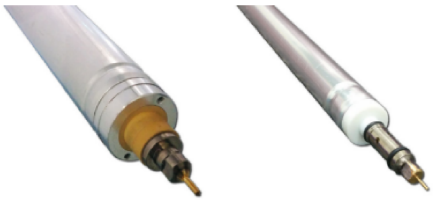

Figure 5: New small monitored drift tubes with a radius of 7.5 mm in comparison to normal monitored drift tubes with a radius of 30 mm. Both use the same gas mixture, wire voltage, and other internal parameters other than the tube radius.
[6]

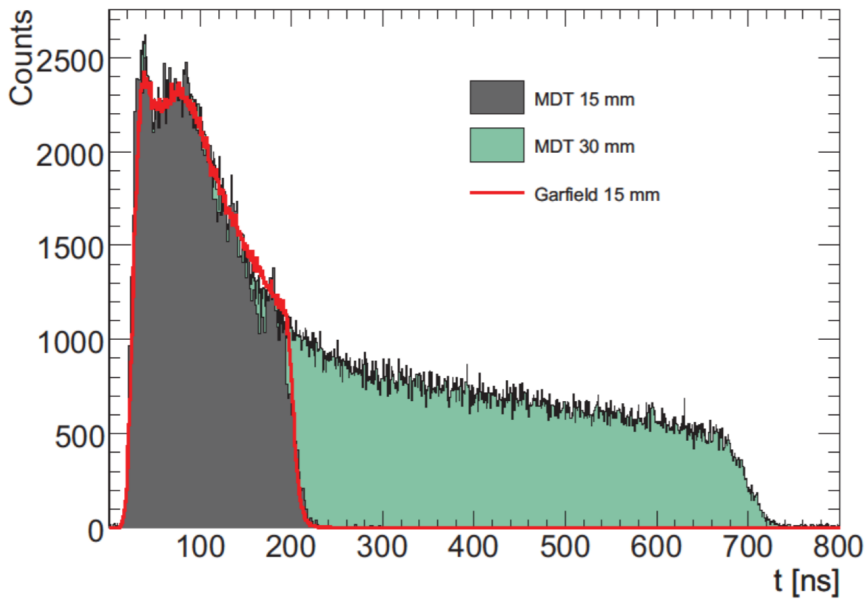

Figure 6: The plot of drift times for an sMDT chamber compared to that of a MDT chamber. The smaller radius of the sMDT chambers results in a maximum drift time of about 175 ns compared to 700 ns or MDT chambers. The red line shows the simulated drift time spectrum from the Garfield program that runs simulations for gaseous detectors. [6].

Currently, the small inner barrel MDT chambers (BIS) have no mounted RPC's, unlike the middle and outer chambers, and sMDT chambers are in production at the University of Michigan in order to replace these chambers. The space that is freed up from this upgrade will be used to mount triggering RPC's to improve the tracking of muons.

While the overall performance of sMDT chambers is superior to MDT chambers for high rates of radiation, sMDT chambers have significantly poorer intrinsic resolution than MDT chambers. Without radiation and space charge effects, the expected resolution of sMDT chambers is 106 $\pm$ 2 μm compared to 83 $\pm$ 2 μm for normal MDT chambers. Dr. Claudio Ferretti calculates that the expected sMDT resolution at the LHC should be approximately 121 μm. The resolution of a chamber is defined to be the average value of the plot of spatial resolution vs drift radius, which is expressed for MDT chambers in figure 7. The conditions in sMDT chamber are the same as MDT chambers, so the expected resolution of sMDT chambers should be the average value of the spatial resolution vs drift radius of an MDT chamber for the first 7.5 mm. The first 7.5 mm of MDT's have poorer resolution than the second 7.5 mm, and thus the resolution of sMDT chambers is poorer than MDT chambers.

In November of 2017, LHC beam data for the sMDT BMG chambers became available, which provided the data necessary to study how the BMG chambers are actually performing within the ATLAS detector. As new chambers, there is still much unknown about their performance, particularly with regards to their working efficiency and resolution. As there are plans to build many more chambers using sMDT technology, establishing high performance and a strong understanding of theses chambers is essential. This paper looks to determine the efficiency and resolution of the BMG chambers and study the factors that influence them in order too evaluate how sMDT function under the working conditions of the LHC.

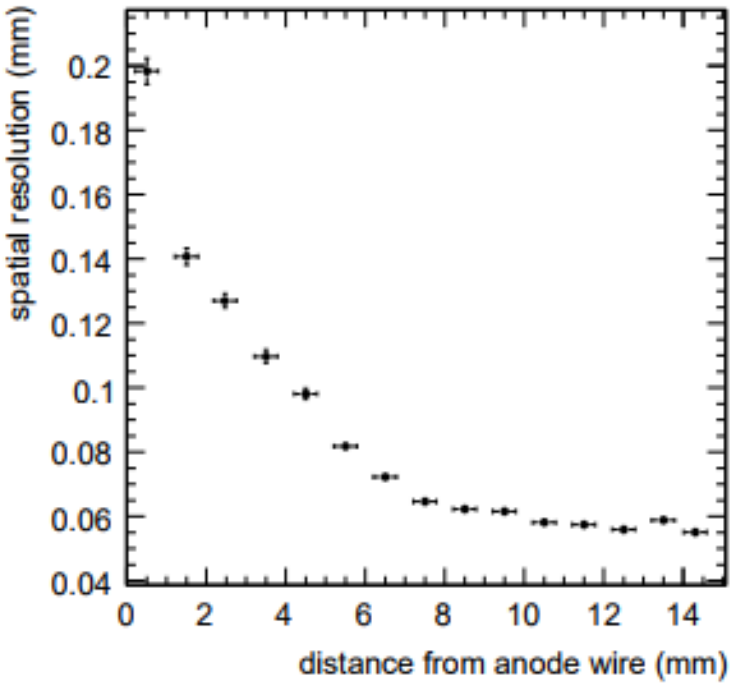

Figure 7: The spatial resolution of an MDT chamber as a function of drift radius. The resolution of the whole tube is the the average value of this plot for the whole radius of the tube. Spatial resolution is poor for low drift radii, which is the reason sMDT's have poorer resolution than MDT chambers [6].

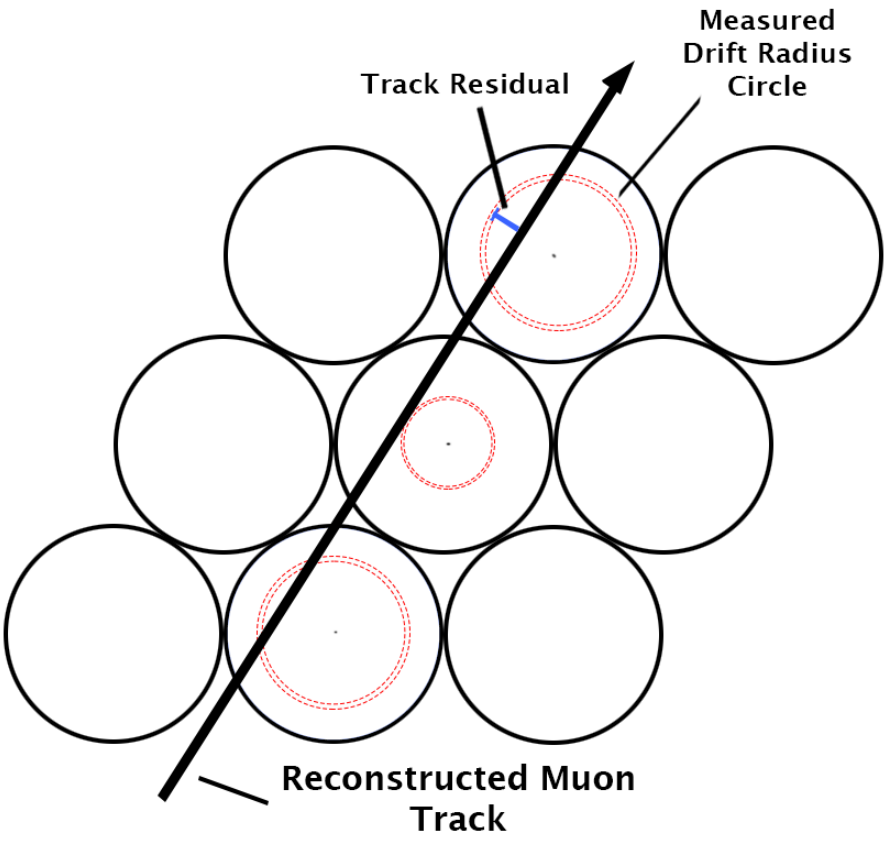

Figure 8: A visualization of the biased residuals for a track. The black arrow represents the reconstructed trajectory of a particle that passes through the tubes. The red dotted circles represent the drift radius circle for each tube where the particle was measured to have passed through the tube. The trajectory is reconstructed based off these drift radii circles, and residual value, shown in blue for the top tube, is the closest distance between the reconstructed track and the drift radius circle for each tube.

2 Resolution

Conceptually, resolution is a measure of how accurately the trajectory of a reconstructed particle can be determined in comparison to its physical trajectory. This quantity is based off of the residual values of a chamber, which comes from the closest distance between a reconstructed track and the physical drift radius of a measured hit. What is called the "biased" residual value given to a certain chamber is found by fitting an equal-mean double Gaussian to the histogram of the residual values for all the tubes in the chamber. The resulting weighted value of σ, which is the average of the two σ values from two Gaussians fit functions, obtained from this fit is the residual value for the chamber. The use of a double Gaussian for this fit is an empirical choice that fits the data. The resolution comes from the biased residual value and the "unbiased" residual value, which is found by calculating the weighted σ value mentioned above multiple times for the tracks created be removing each track hit one at a time and refitting a new track.

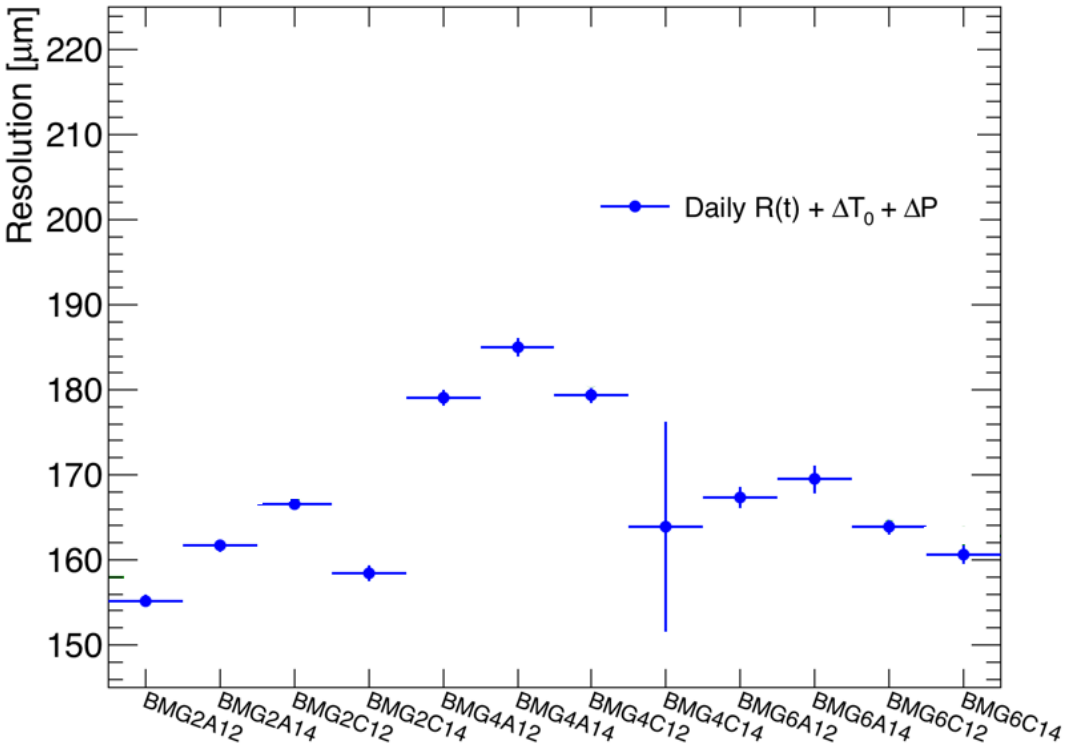

Figure 9: Chamber resolution of the 12 BMG chambers in 2017.

The resolution can then be found from [11]

$$Resolution = \sqrt{\sigma^2_{biased} + \sigma^2_{unbiased}}$$

For the most accurate resolution values, adjustments must be made based on the RT function, the minimum drift time (ΔT_0), and the pressure (ΔP) and temperature of the gas. RT functions, which convert the drift time measured by MDT chambers into a drift radius, are functions of the gas conditions within each tube. Conditions throughout the ATLAS detector, such as temperature, vary greatly, so each chamber has its own RT functions that are adjusted to account for the appropriate conditions. By adjusting for these parameters and using the definition of resolution outlined above, Dr. Ferretti calculated the resolution of all 14 sMDT chambers (12 BMG and 2 BME) using 2017 data, and the results are displayed in figures 9 and 10. The resolution of the BME chambers was also calculated for 2017.

As is evident from figure 9 and 10, the resolution of the BMG chambers, and all sMDT chambers for that matter, is far larger than the expected 121 μm value. In addition to this, there is large fluctuation in the resolution of the different BMG chambers as great as 30 microns (as is the case between the BMG2A12 and BMG4A14 chambers). This should not be the case as all the BMG chambers were made using the same materials and procedures in the same facility and should have essentially the same resolution. The track residual values found from high statistic combined plots of data from November 2017 corroborate this high resolution among the BMG chambers ranging from 160 to 190 microns.

Several different variables were studied to measure their effect on the resolution of these

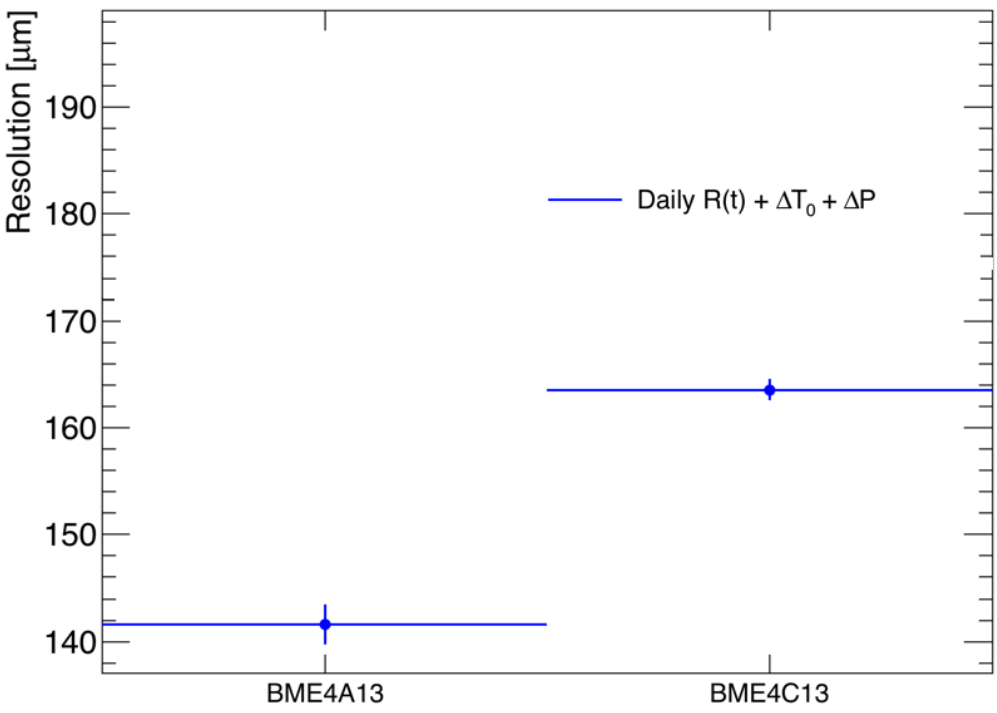

Figure 10: Chamber resolution of the BME chambers in 2017, minimized using the appropriate RT functions, and ΔT_0 and ΔP values.

chambers in order to look for the cause or causes that were accounting for 40-50% poorer resolution than what these small drift tubes were designed for. Firstly, the BMG chambers were known to have high amounts of electrical noise, as is shown in figure 11. Noise hits are especially common near the edges of the chambers and along the cutouts, such as is the case in figures 13 and 14. For BMG chambers, these noise hits can most commonly be identified as hits that have either a negative drift time value or a drift time value greater than 190 ns, or hits with ADC (analog-to-digital converter) values less than 200 ticks. It is often the case that these non-physical noise hits get fit to tracks and disrupt the quality of the track fits. By sorting out track fits that have these qualities, the track residuals with and without these noise hits could be compared to see some of the impact that these noise hits make on the overall residuals.

Removing these noise hits after reconstruction seems too have little to no effect on plots of residuals. An example of the residual plots and residual vs drift radius plots with and without noise hits for the BMG2A12 is shown in figure 12. However, this is a bit misleading; the noise hits that were identified were already used for track fits, which means that the track fit quality is still disrupted regardless of these hits being included into the histograms. To test the whole effect of these noise hits on the residuals and by extension the resolution, these points would have to be filtered out and then refit so that the fit is not affected by them.

Another possible contributer to the poor resolution were the old RT functions, which gives an extrapolated drift radius from measured drift time, for sMDT chambers. The RT functions used for sMDT chambers were unnecessarily defined between -15 mm and 15 mm,

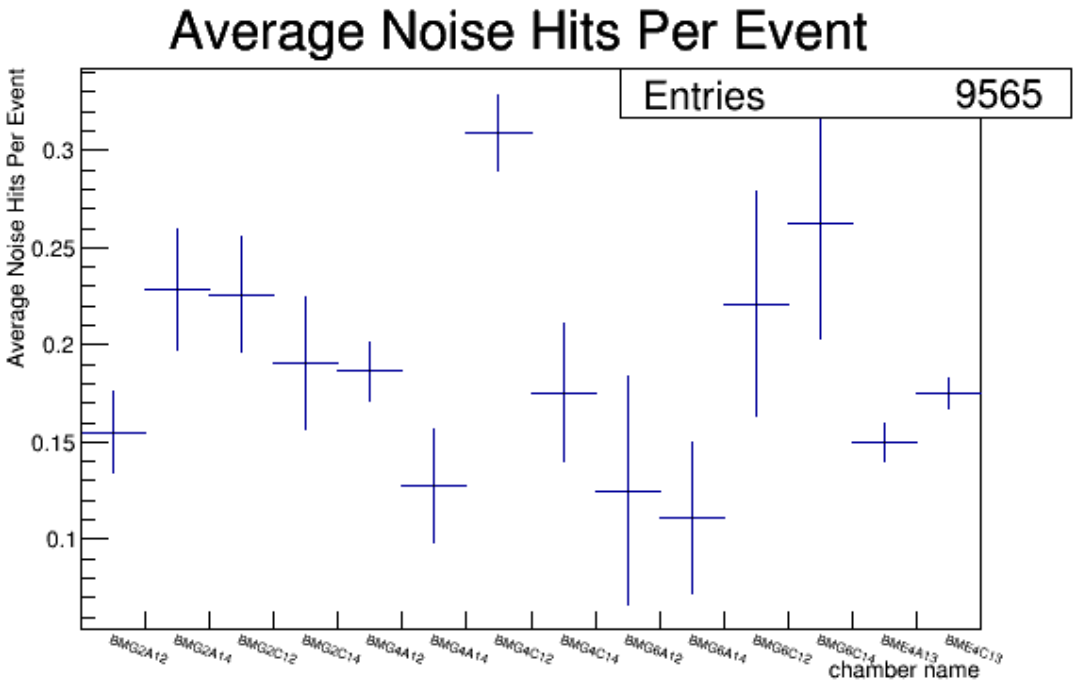

Figure 11: The number of noise hits, defined as hits with drift time values not between 0 and 190 ns, and ADC values under 200 ticks, that were fit to tracks per event for each of the sMDT chambers in the 338675 run. This plot shows that hits with non-physical drift times and ADC values are being fit to tracks, which could be a factor causing the poor resolution that we are seeing in the sMDT chambers.

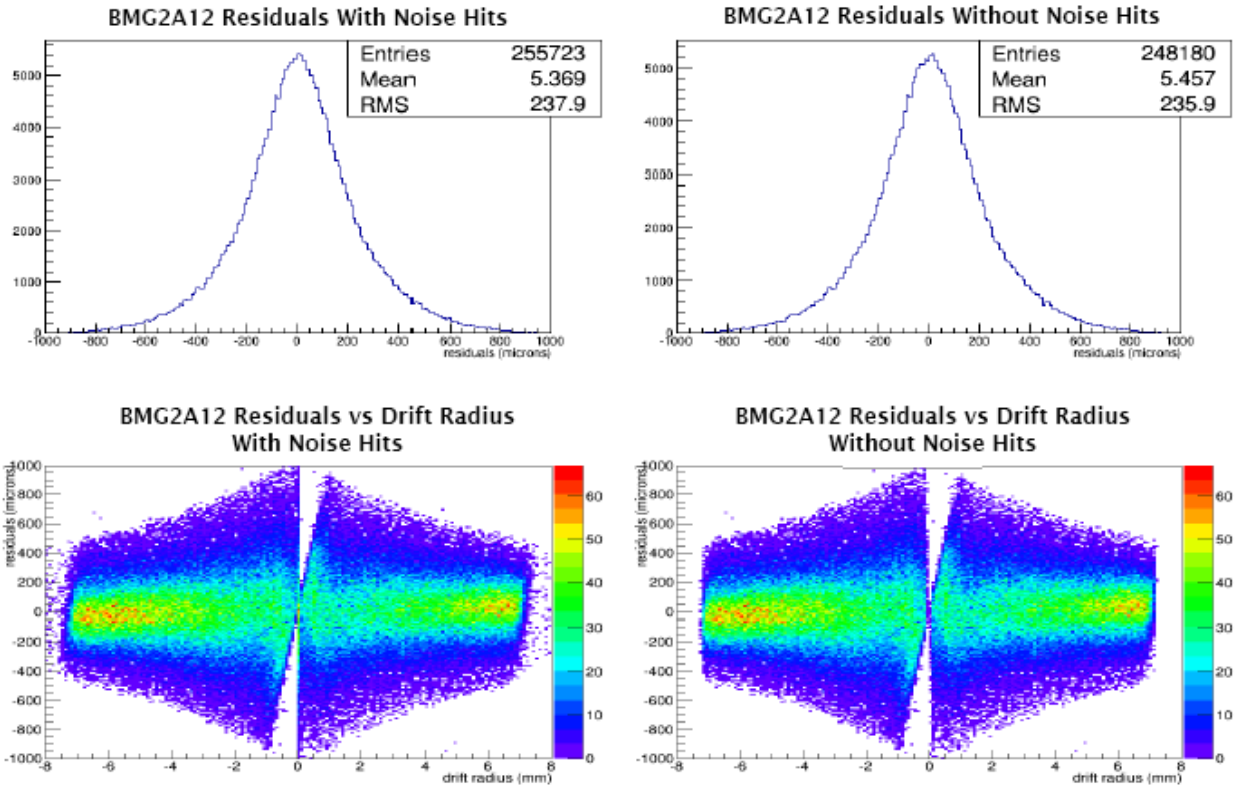

Figure 12: The plots of the track residuals and track residuals vs drift radius with and without filters on ADC/drift time for the BMG2A12 chamber from run 339849. The plot of track residuals shows the distribution of residual values in the BMG2A12 chamber with the y-axis showing the number of track hits with a certain residual value. The residual vs drift radius plot shows the distribution of residual values at different drift radii. Little to no change in residuals was achieved by filtering out noise hits, which is evident in these plots.

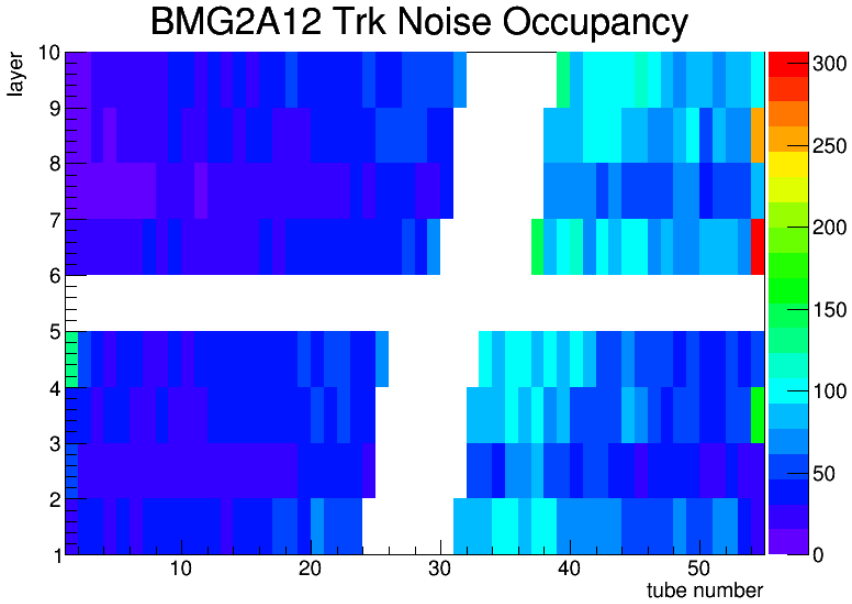

Figure 13: This plot shows the number of noise hits, defined as hits that are not in tracks or segments, in each tube, or noise hit occupancy, in the BMG2A12 chamber during the 201711 run. For these types of plots, the y-axis denotes tube layer, and the x-axis denotes the tube number within that layer. The lack of hits between layers 5 and 6 represents the spacer gap between multilayers on MDT and sMDT chambers. Furthermore, the lack of hits in the diagonal region at the center of the plot is caused by the cutout of the chamber, which is a region on each BMG chamber where no tubes are present for mechanical purposes. Notice the tubes on the right edge of the chamber that detect a high amount of noise hits in comparison to the rest of the tubes.

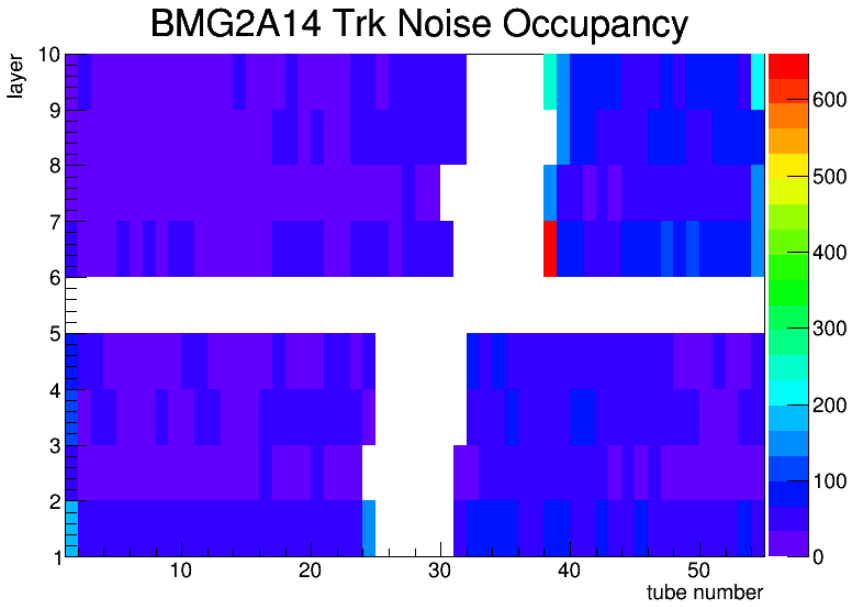

Figure 14: High amounts of noise hits found on the tubes bordering the cutout of the BMG2A14 chamber from combined run data from November 2017.

which allowed for measured non-physical drift times to be converted to non-physical drift radii [3]. Dr. Diehl changed the range of the RT functions for sMDT chambers so that they were only defined for the physical -7.5 mm to 7.5 mm range, which prevented any non-physical drift radii being registered. With the edited sMDT RT functions, the 339849 run was reprocessed by Dr. Diehl and only small changes were found. A comparison between the track and segment residuals for the BME4A13 chamber using both the original and updated RT functions is shown in figure 15. The residual value for both tracks and segments were generally unchanged or negligibly better than with the MDT RT functions. Once again, there appears to be no relation between the poor resolution and the RT functions.

We also compared the drift time and ADC plots for each multilayer, as differences in these could point to a problem with gas distribution. However, we found no significant difference in the track drift time and ADC plots.

Despite multiple studies into possible causes, the origin of the poor resolution of the sMDT chambers is still unknown. Further study into the effect of noise on the chambers might yield more fruitful results, particularly if ADC and drift time cuts are made before reconstruction to weed out the usual electrical noise hits. This would make a more concrete comparison between residuals with noise hits and residuals without them, as the noise hits would not be present during reconstruction to affect the position of tracks.

Another possible reason could be that the chambers were not built to meet the required wire location precision (25 microns). This will be investigated at Michigan in the sMDT R&D project for ATLAS high-luminosity muon detector upgrade project.

[3] That is, drift radii that that are greater than 7.5 mm or less tha -7.5 mm

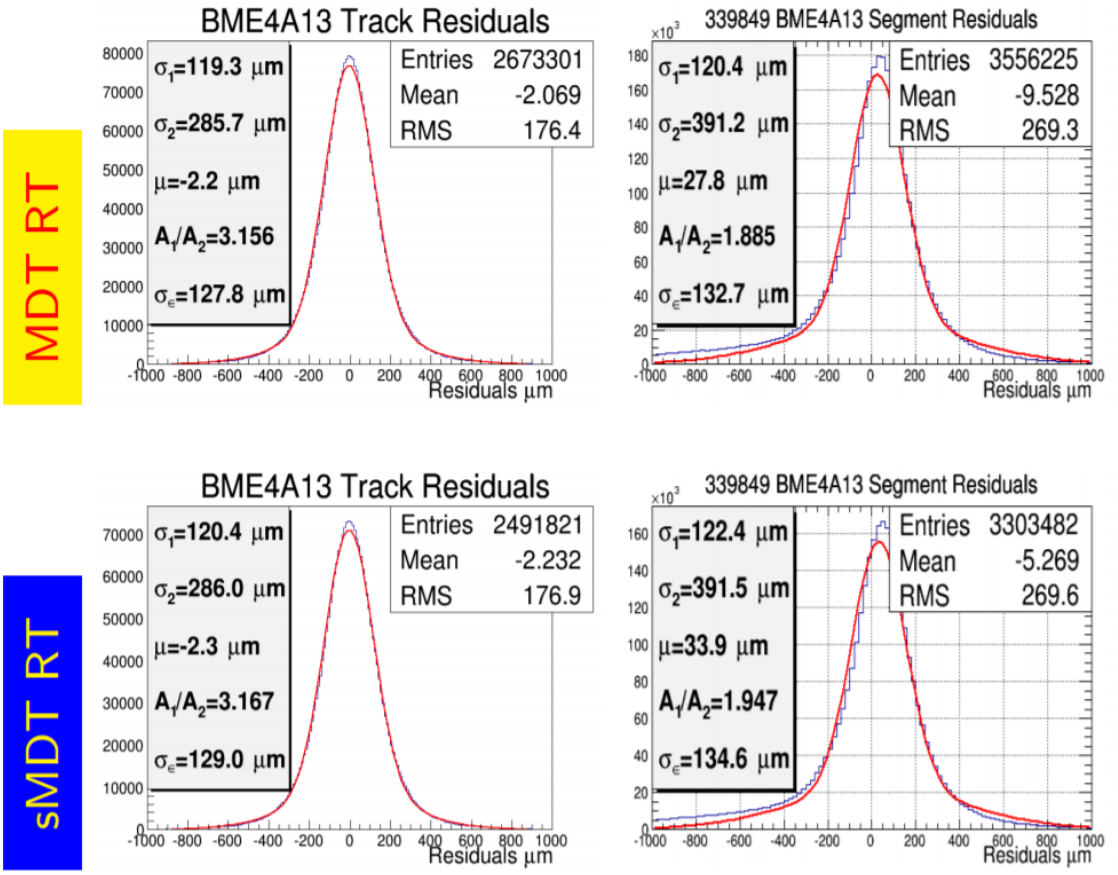

Figure 15: Comparison of the segment and track residual plots for both MDT and sMDT RT functions showing the negligible change between the two.
[9]

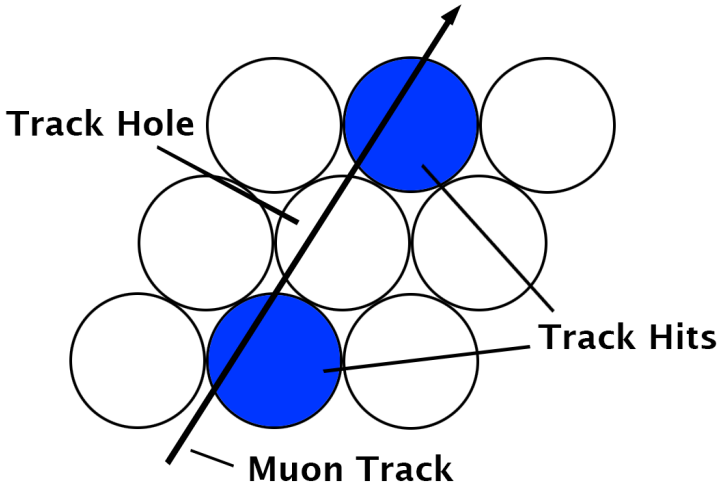

Figure 16: Visualization of what a hole looks like on a reconstructed track where tubes that are shown in blue have registered hits and white tubes have not.

3 Efficiency

Muon trajectory reconstruction is not usually a perfect process, as we saw before where noise hits were being misidentified as track hits and fit to tracks. On the hardware side, drift tubes do not always work as they should, and there are times when Athena expects a certain tube on a track to register a physical particle hit, but in reality there were no measured hits on that tube. This lack of a hit is referred to as a track 'hole', which is visualized in figure 16. Athena can also identify other track hits as delta rays, which are ionized electrons with a high enough energy to escape their primary beam and induce a hit, and outliers, which are hits that are initially thought to be track hits that turn out to be greater than 3σ from the track later on in the reconstruction. Tracks holes most commonly occur due to physical hits passing through drift tubes during the 790 ns MDT dead time prompted by background noise or delta ray electrons. At higher luminosities, the dead time can also be prompted by other particles resulting from the collision, which is why tube efficiency decreases with higher rates of radiation.

When describing the performance of chambers, a useful quantity to define is tube efficiency, which is the probability of a tube registering a hit when a fitted track passes through the tube. Tube efficiency is particularly useful to look at because it is a measure of both the quality of the drift tube hardware and the quality of track reconstruction. Poor tube efficiency can be the result of high noise or other aspects of the hardware not functioning correctly, or it could also be the result of poor reconstruction that predicts tracks passing through tubes where no particle actually passed through. Using calibration stream data processed by Athena, we made a study of the tube efficiency based on the definition,

$$\epsilon = \frac{trackhits}{trackhits + holes}$$

[11]

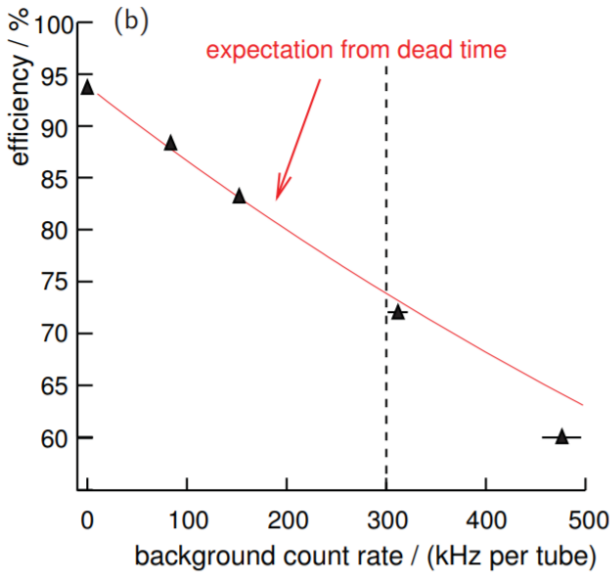

Figure 17: The efficiency of an MDT tube as a function of the rate of radiation. The red line indicates the expected efficiency taking into account only the read-out electronics with a dead time of 790 ns. At 300 Hz/cm^{-2}, the highest expected rate of radiation per tube, the tube efficienc drops to 72% in comparison to 96% with no radiation. [5].

For MDT chambers, the expected efficiency starts at slightly under 95% in the absence of background radiation, and decreases to nearly 60% for a count rate of 500 kHz, as expressed in figure 17. In principal, sMDT tubes are expected to function with higher efficiencies for high count rates as the maximum drift time and dead time are much lower than MDT tubes.

Using the track data from Athena from calibration stream in November and December 2017, we attempted to calculate the efficiency of the BMG chambers using the definition mentioned above and identified a strange pattern in sMDt tube efficiencies. In plots of the efficiency as a function of tube number [4], which begins with the first tube of the first layer and runs to the last tube of the last layer, we found a strange, periodic pattern in the efficiency as opposed to a roughly flat plot that we would expect. Figure 18 shows an example of this plot for the BMG2A12 chamber, where the efficiency switches back and forth between about 99% and 70%. Interestingly, this pattern was found for all sMDT chambers, BME and BMG, yet not for normal MDT chambers. We found that the cause of this pattern is because of the existence of a large number of holes in certain ranges of tube numbers shown in figure 19 for the BMG2A12 chamber. Upon further investigation, we realized that the even layers of the sMDT chambers were found to have large amount of holes, nearly a factor of ten more, in comparison to the even layers. This can be seen in figure 20, which shows the track hole occupancy plot for the BMG2A12 chamber.

[4]for the BMG chambers, tube number ranges from 1 to 432.

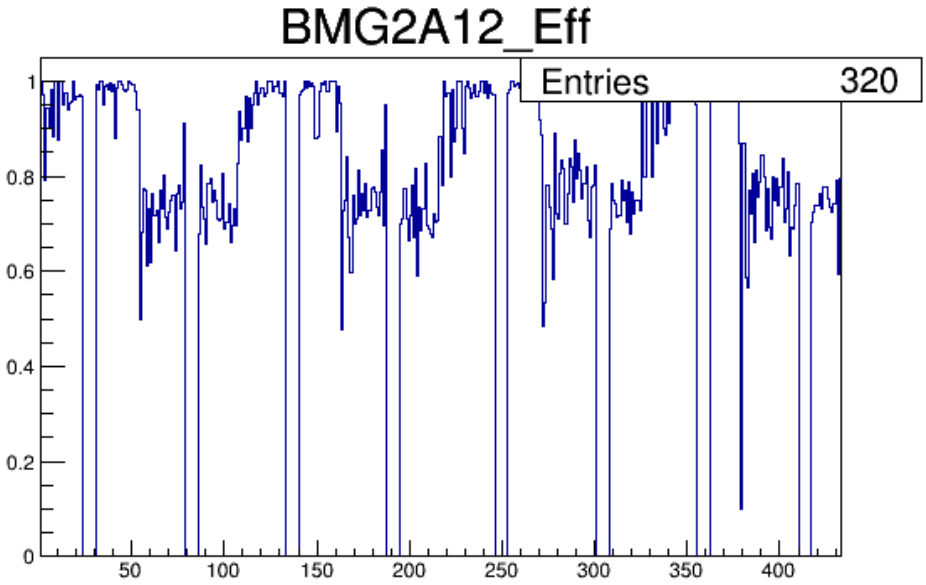

Figure 18: An example of the periodic pattern in the plot of tube efficiency vs tube number. Note that the tubes with apparent efficiencies of zero correspond to the cutout region of the chamber where there are no tubes.

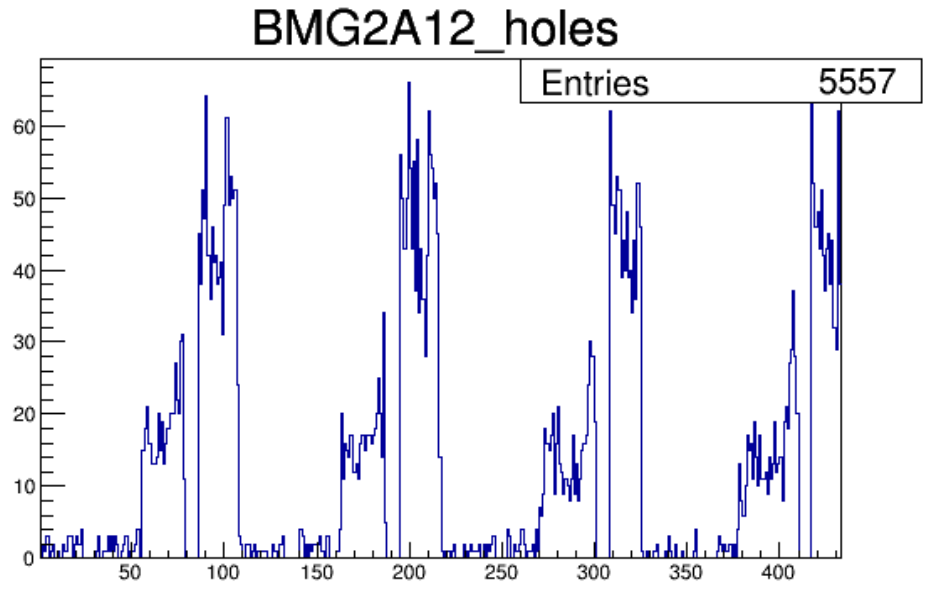

Figure 19: The periodic pattern of track holes found in the BMG2A12 chamber. The x-axis is the tube number, and the y-axis shows the track hole hit count.

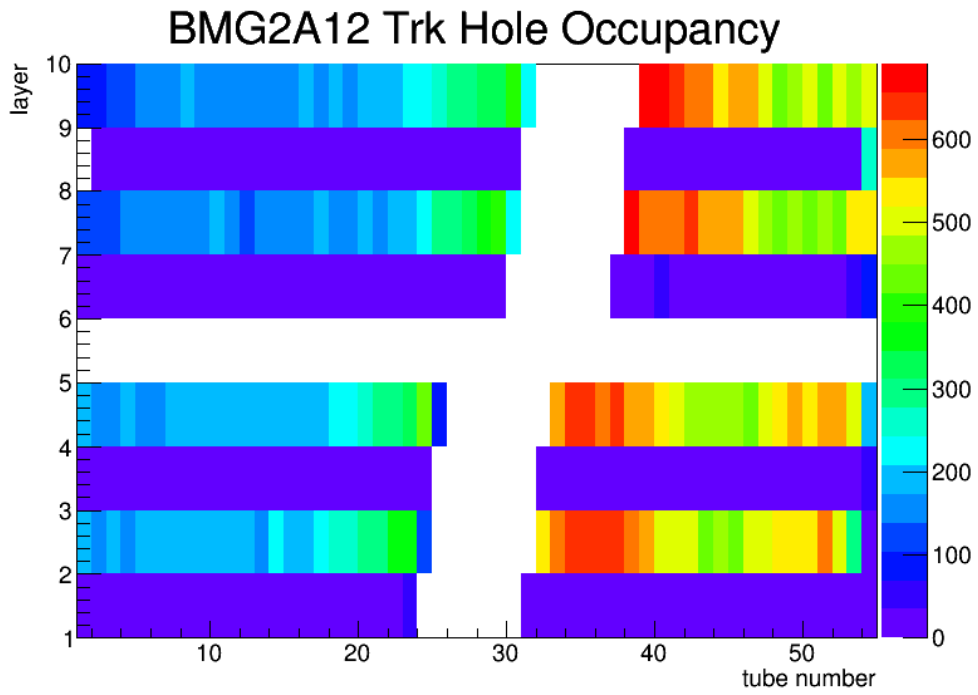

Figure 20: Occupancy plot of the number of holes in each layer after several runs. Even layers received large numbers of holes whereas the odd layers had very few. The white gaps in the middle of the chamber are cutouts in each multilayer

4 Even Layered Tracking Holes

We first examined the drift radius, residual, and residual vs drift radius plots for the even and odd layers of the sMDT chambers in order to look for differences that could explain why we are seeing such different amounts of holes between the even and odd layers. However, there was no significant differences between these plots other than a very small shift in the residual plots of less than 30 microns for some of the chambers. To investigate the circumstances in which these large number of holes were seen on the even layers of the BMG chambers were occurring, we wrote a program to give a visual representation of the track hit occupancy of events that have high numbers of holes. The color of the hit denotes whether it is a hit on track, hole, outlier, or delta ray. Two such events are visualized in figures 21 and 22.

In studying these event printouts, there was a clear pattern of holes almost always being located next to hits on track, which is also the case with the holes in figures 21 and 22. To look more into this, we took a look at the percentage of holes that were next to a hit on track versus those next to another hole or not next to any other hit types on the same layer. This analysis revealed the fact that about 90% of track holes are located in the even layers, and roughly 90% of these holes in the even layers are located next to a hit in track.

Holes have have no drift radius within Athena as there is no physical hit to get a drift time from to then convert to a drift radius, but Athena does give what is ostensibly the absolute value of the distance from the track to the center of tubes that it deems to be holes. We studied this implied drift radius for the several categories of track holes for each of the

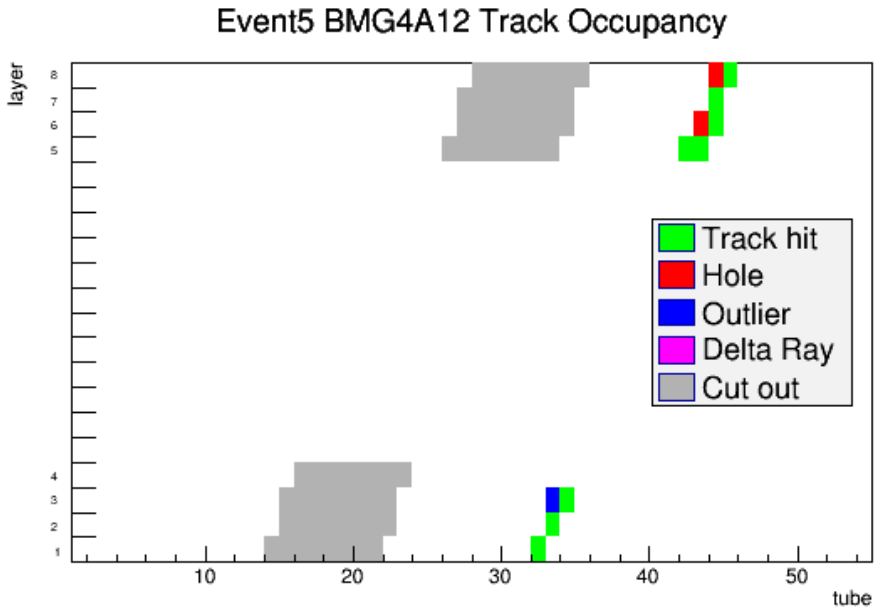

Figure 21: An event plot of the BMG4A12 chamber during event number 5 of the 338675 run. Notice the holes on the even layers that are next to hits on track.

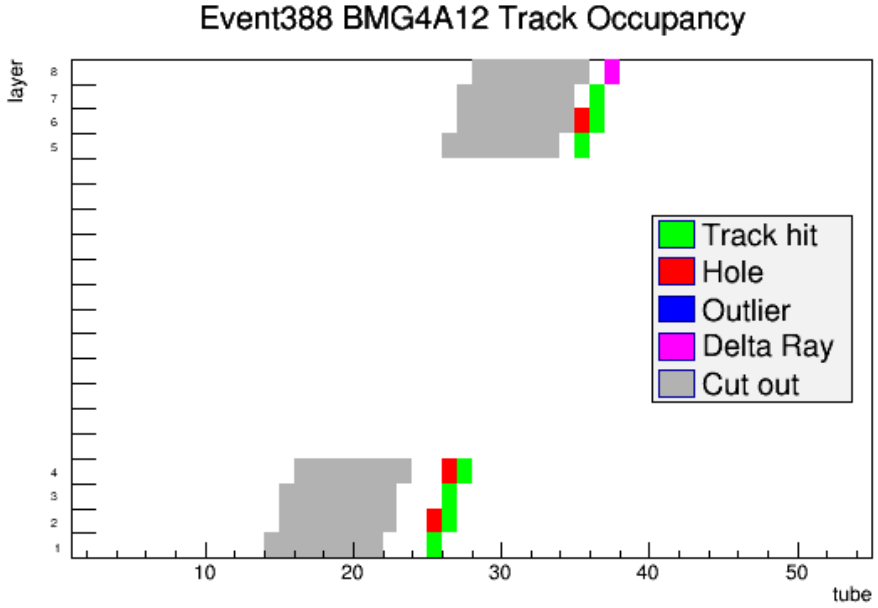

Figure 22: The BMG2A14 chamber occupancy during event 881 of the 338675 run. The holes on layers 2, 4, and 6 are all located adjacent to hits on track.

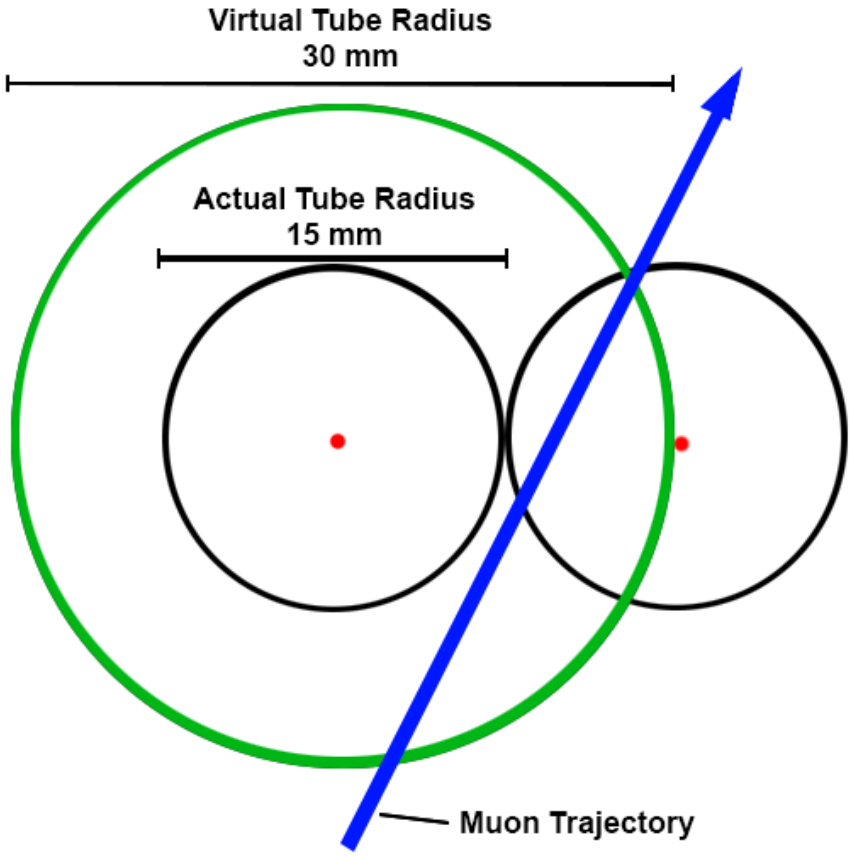

Figure 23: In this diagram, the tube radius of the sMDT tube is expected to be 30 mm in Athena, so when a muon passes through a neighboring tube, it expects that it should also receive a hit. Since the muon never actually passes through the tube, it never registers a hit, and thus the reconstruction software tags it as a track hole. This would explain the non-physical drift radii that we are seeing in the drift radii histograms.

chambers, mainly holes adjacent to hits on track, holes located on even layers, holes adjacent to hits on track that are on even layers, etc. These plots showed that the drift radii for the holes that we are seeing are almost all located in the non-physical range between 7.5 mm and 15 mm. An example of these plots can be seen in figure 24. Combined with the fact that the vast majority of track holes are adjacent to hits on track, this discovery leads us to believe that the reconstruction software is treating the even-layered tubes in sMDT chambers as MDT tubes with diameters of 30 mm. In this case, a particle would pass through a tube and be registered as a hit on track. The neighbor tube closest to the trajectory of the particle is treated as an MDT chamber, so the reconstruction software believes that this particle also passes within this tube's radius, and thus, seeing that it registered no physical hit, tags it as a hole. This is represented visually in figure 23

This might point to a drift tube radius parameter in the Athena code that is hard-coded for MDT chambers. The fact that we are only seeing this issue on the even layers might suggest that there are drift radius parameters for both even an odd layers, and only the even layered parameter is hard coded to MDT chambers. Alternatively, the fitting algorithm that

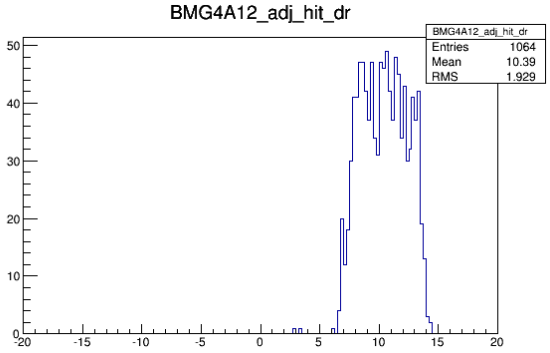

(a) Histogram of the drift radius (in mm) of track holes adjacent to hits on track.

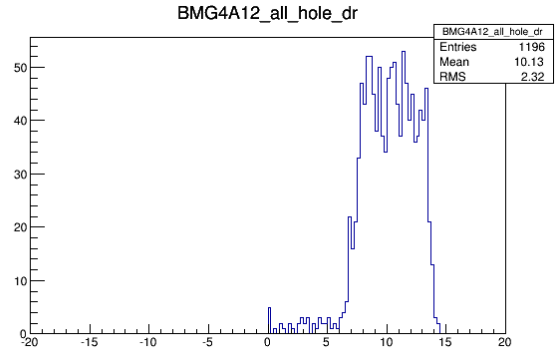

(b) Histogram of the drift radius (in mm) of all track holes for the BMG4A12 chamber.

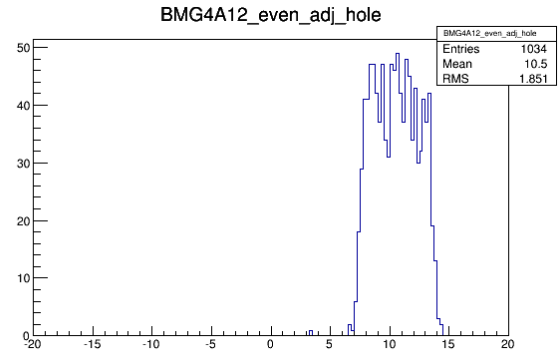

(c) Histogram of the drift radius (in mm) of the track holes located on the even layers that are adjacent to a hit on track.

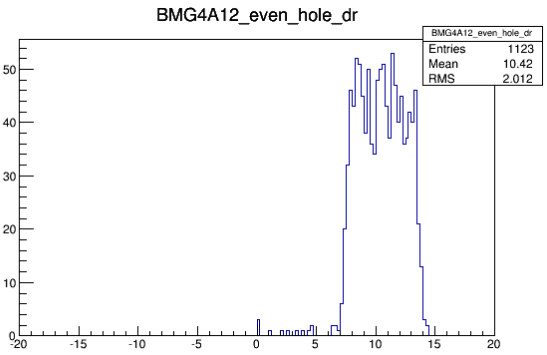

(d) Histogram of the drift radius (in mm) of all the holes located on the even layers of the BMG4A12 chamber.

Figure 24: Different drift radius histograms for the BMG4A12 chamber during the 338712 run that demonstrate the circumstances of the even layered holes. Nearly 90% of holes are located in the even layers, and about 90% of these holes are adjacent to a hit on track. Furthermore, the overwhelming majority of track holes had non-physical drift radii; greater than 7.5 mm in chambers that only go out to 7.5 mm.

Athena uses to fit tracks might treat the even and odd layers differently in reconstruction, resulting in only holes in the even layers.

Research engineer Tiesheng Dai at CERN suggested that the non-physical drift radii seen in the histograms in figure 24 could be explained by an incorrect tube layer offset. The tube layers are offset from each other by half the width of one tube so that they fit together tightly. Having the incorrect tube offset would shift the drift radius histogram by 7.5 mm. However, in checking the layer offset, we found that it matched the convention provided by Tiesheng Dai, so this does not appear to be the case.

What we have been able to find so far seems to be strong evidence for an outdated reconstructon parameter in the Athena code. The next step we will take is to contact software experts that are familiar with the code for Athena in order to try to locate this hard-coded parameter. Another important note is that the excess of holes in the even layers does not appear to be affecting the resolution of the BMG chambers, as Dr. Ferretti uses his own code to make track fits and calculate resolution, and he does not see the large amount of holes in the even layers that is present in calibration stream.

5 Summary

Despite the expected spatial resolution of 120 μm for sMDT chambers, the resolution that we are actually seeing with LHC beam data ranges between 150 and 185 μm for the BMG chambers and slightly lower for the BME chambers. Through the studies that we conducted, there appears to be no correlation between the poor resolution and the RT functions, nor did we find any signs of gas distribution problems that would contribute to the poor resolution. What remains a possible source of the poor resolution is the large amount of noise hits that are often fit to tracks. To really see the effect of these noise hits on the resolution, a cut for ADC and TDC values would have to be made to exclude non-physical hits and then be reprocessed.

No useful data regarding the efficiency of the BMG chambers was able to be found in light of the of the problem with reconstruction that we found. Through analyzing event displays and viewing the drift radii of the track holes in different circumstances, we have found strong evidence that suggests that MDT parameters are being used for the sMDT chambers in the even layers. Contacting ATLAS software experts and searching through the Athena code for hard-coded MDT parameters might be necessary in order to test our hypothesis and verify the origin of this problem.

This thesis work is just a foundational investigation of the performance of the BMG chambers, but it provides the ATLAS muon team with valuable information that can aid in future chamber design, construction techniques, and calibration approaches for the upcoming high-luminosity upgrades for which many new sMDT chambers will be made. Through my study, both hardware related and software problems on these new chambers were identified, and some remain to be understood. For this reason, great efforts must be made in detector construction and calibration to reach the design goals of the ATLAS experiment in preparation for the upcoming Long Shutdown 2 during 2019 and 2020. Enormous efforts have been and will be made to understand and improve the performance of the sMDT chambers in terms of tracking resolution and efficiency. In conducting this study of the BMG

chambers, I have gained strong experience working on performance studies of the sMDT and MDT chambers using p-p collision data from the LHC, strengthened my understanding of the ATLAS experiment, and learned about how high energy physics is studied at the LHC.

Acknowledgements

I would like to thank Professor Bing Zhou for guiding and teaching me during my research with the ATLAS experiment. I would also like to thank Dr. Edward Diehl and Dr. Claudio Ferretti, who are the muon calibration experts that provided me detailed help during my thesis research. Lastly, I would also like to thank my peer students Cooper Wagner and Ezra Lesser for their insights regarding the ATLAS detector.

References

[1] The ATLAS Collaboration, 2008 *The ATLAS Experiment at the CERN Large Hadron Collider*

[2] The ATLAS Collaboration, July 14, 2016 *The ATLAS Experiment at the CERN Large Hadron Collider*

[3] The ATLAS Collaboration, June, 2013 *ATLAS New Small Wheel Technical Design Report*

[4] C. Ferretti, H. Kroha *Upgrades of the ATLAS Muon Spectrometer with sMDT Chambers.* the ATLAS Muon Collaboration

[5] M. Deile, et al. *Resolution and Efficiency of the ATLAS Muon Drift-Tube Chambers at High Background Rates*

[6] The ATLAS Collaboration, CERN *Support document for the Muon Phase-II upgrade Initial Design Review.* July 14, 2016

[7] B. Bittner et al. *Performance of drift-tube detectors at high counting rates for high-luminosity LHC upgrades.* Nucl. Instr. Meth. A 732 (2013) 250.

[8] E. Etzion, et al., 2004 *The Certification of ATLAS Thin Gap Chambers Produced in Israel and China*

[9] Edward Diehl, Ethan Cannaert, The University of Michigan, February 22, 2018 *BMG Reconstruction: MDT RT vs sMDT RT*

[10] Ph. Gadow, O. Kortner, H. Kroha , R. Richter Max-Planck-Institut fur Physik, F ohringer Ring 6, D-80805 Munich, Germany *Precision Muon Tracking Detectors for High-Energy Hadron Colliders*

[11] R.K. Carnegie et al, Nucl. Instrum. Meth. A538 (2005) 372-383